Journal of Neurochemistry

JOURNAL OF NEUROCHEMISTRY | 2009 | 108 | 1226–1236 doi: 10.1111/j.1471-4159.2009.05871.x

Aminoglycoside-induced histone deacetylation and hair cell death in the mouse cochlea

Fu-Quan Chen,[1] Jochen Schacht and Su-Hua Sha

Kresge Hearing Research Institute, Department of Otolaryngology, University of Michigan, Ann Arbor, Michigan, USA

Abstract

Post-translational modification of histones is an important form of chromatin regulation impacting transcriptional activation. Histone acetyltransferases, for example, acetylate lysine residues on histone tails thereby enhancing gene transcription, while histone deacetylases (HDACs) remove those acetyl groups and repress gene transcription. Deficient histone acetylation is associated with pathologies, and histone deacetylase inhibitors have been studied in the treatment of cancer and neurodegenerative diseases. Here we explore histone acetylation in cochlear sensory cells following a challenge with gentamicin, an aminoglycoside antibiotic known to cause loss of auditory hair cells and hearing. The addition of the drug to organotypic cultures of the mouse organ of Corti decreased the acetylation of histone core proteins (H2A Ack5, H2B Ack12, H3 Ack9, and H4 Ack8) followed by a loss of sensory cells. Protein levels of HDAC1, HDAC3 and HDAC4 were increased while the histone acetyltransferases such as CREB-binding protein and p300 remained unchanged. We next hypothesized that protecting histone acetylation should prevent cell death and tested the effects of HDAC-inhibitors on the actions of gentamicin. Co-treatment with trichostatin A maintained near-normal levels of acetylation of histone core proteins in cochlear hair cells and attenuated gentamicin-induced cell death. The addition of sodium butyrate also rescued hair cells from damage by gentamicin. The results are consistent with an involvement of deficient histone acetylation in aminoglycoside-induced hair cell death and point to the potential value of HDAC-inhibitors in protection from the side effects of these drugs.

Keywords: cochlear explant, gentamicin, histone acetyl transferase, histone deacetylase inhibitors, ototoxicity.

J. Neurochem. (2009) **108**, 1226–1236.

Post-transcriptional modification of histones modulates gene transcription through effects on tertiary chromatin structure, differentially affecting the access of the transcriptional machinery to sections of DNA. The N-terminal tails of the core histones, including H2A, H2B, H3 and H4, contain specific amino acid sequences for acetylation, methylation, phosphorylation, ubiquitination and sumoylation (Sadri-Vakili and Cha 2006). Histone acetyltransferases (HATs), add acetyl groups to lysine residues, thereby facilitating the binding of transcription factors to nucleosomal DNA and activating transcription while histone deacetylases (HDACs) remove acetyl groups promoting chromatin condensation and reduced transcription (Marks *et al.* 2001). These changes are implicated in a variety of biological functions such as transformation, differentiation, cell survival, and cell death (de Ruijter *et al.* 2003; Marks *et al.* 2004).

Epigenetic modifications including deficient histone acetylation have been observed in many progressive neurodegenerative conditions such as Huntington's disease (Taylor and Fischbeck 2002). Aberrations of the acetylation homeostasis mostly result from a loss of HATs like CREB-binding protein (CBP) or p300, and HDAC-inhibitors can be used in order to restore balance and ameliorate the disorders (Saha and Pahan 2006). For example, HDAC-inhibitors increase histone acetylation in hippocampal tissue *in vivo* and restore learning ability and memory to a mouse model of neurodegenerative disease (Fischer *et al.* 2007). They also diminish neuroinflammation and neuron apoptosis and improve neurological performance after cerebral ischemia in animals

Received September 15, 2008; revised manuscript received November 20, 2008; accepted December 12, 2008.

Address correspondence and reprint requests to Su-Hua Sha, Kresge Hearing Research Institute, Medical Sciences Bldg I, Room 5315, 1150 West Medical Center Drive, Ann Arbor, MI 48109-5616, USA.
E-mail: shasha@umich.edu

[1]The permanent address of Fu-Quan Chen is the Department of Otolaryngology-Head and Neck Surgery, Xijing Hospital, Fourth Military Medical University, Xi'an 710032, China.

Abbreviations used: CBP, CREB binding protein; CREB, cAMP-response element binding protein; DMSO, dimethyl sulfoxide; GAPDH, glyceraldehyde 3-phosphate dehydrogenase; GTTR, gentamicin linked to Texas Red dye; HAT, histone acetyltransferase; HDAC, histone deacetylase; PBS, phosphate-buffered saline; TSA, trichostatin A.

(Kim *et al.* 2007). In cancer therapy HDAC-inhibitors are being investigated for their ability to influence the expression of 7–10% of transcribed genes in cancer cells and to induce cell cycle arrest and senescence (Xu *et al.* 2007).

Four classes of mammalian HDACs have been identified and classified based on homology to yeast HDACs (Gao *et al.* 2002; Morrison *et al.* 2006). Class I HDACs, including HDAC1, 2, 3, and 8, are nuclear proteins expressed in most tissues and cell types, and function as transcriptional repressors. Class II HDACs include HDAC4, 5, 6, 7, 9, and 10, and function as a shuttle between cytoplasm and nuclei. Class III, sirtuins, requires NAD^+ for its enzymatic activity and class IV, HDAC11, has conserved residues in the catalytic core region shared by classes I and II. Commonly used HDAC inhibitors such as trichostatin A (TSA) efficiently block all class I and II HDACs.

In the studies presented here we explore whether a histone acetylation imbalance may also be involved in the 'ototoxic' actions of aminoglycoside antibiotics. Treatment with aminoglycoside antibiotics can lead to auditory or vestibular deficits in 10–20% of patients, curtailing their clinical use (Forge and Schacht 2000). Despite their toxic side effects, drugs including gentamicin, kanamycin or tobramycin are in use worldwide to combat serious gram-negative infections, such as prophylaxis in cystic fibrosis, and in the treatment of tuberculosis. Emerging applications are associated with ability of the drugs to suppress premature stop codons and thus serve as potential therapeutics for a variety of genetic diseases (Hermann 2007; Hainrichson *et al.* 2008).

Animal models have linked aminoglycoside ototoxicity to oxidative stress causing the loss of hair cells, the sensory cells in the cochlea and the vestibular system (Forge and Schacht 2000). Cochlear sensory cells include the inner hair cells and three rows of outer hair cells which are located in the auditory end organ, the organ of Corti. Inner hair cells are the primary sensory cells that convert the mechanical acoustic input into receptor potential and release of neurotransmitters, triggering action potentials that are carried to the auditory centers in the brain by the spiral ganglion neurons. The major function of outer hair cells is to enhance the performance of the cochlea, particularly at low intensities of sound. Surrounding supporting cells include the inner and outer pillar, Deiters', Hensen's and Claudius' cells, but their function remains largely unexplored.

Hair cell responses to ototoxic challenge are complex and involve both homeostatic reactions (Jiang *et al.* 2005) and cell death pathways of necrosis and caspase-dependent and caspase-independent apoptosis (Jiang *et al.* 2006b). Recent studies have also shown that treatment of mice with kanamycin increased the levels of phosphatidylinositol 4,5-bisphosphate and decreased the acetylation of histone H3 in the nuclei of outer hair cells (Jiang *et al.* 2006a). We now hypothesize that kanamycin-induced hypo-acetylation of histones may be associated with aminoglycoside-induced hair cell loss and that consequently, restoration of histone acetylation with HDAC-inhibitors should rescue inner ear hair cells. The present study therefore investigates acetylation of histone core proteins in the organotypic culture of organ of Corti in response to a gentamicin challenge and assesses the effects of HDAC-inhibitors.

Materials and methods

Materials

Polyclonal rabbit antibodies against HDAC1, HDAC3, HDAC4, HDAC6, and against acetyl-histone H3 (Lys9), acetyl-histone H2A (Lys5), acetyl-histone H2B (Lys12), acetyl-histone H4 (Lys8), and against histone H2A, histone H3 as well as corresponding secondary antibodies, radioimmunoprecipitation assay (RIPA) buffer (catalogue number: 9806) were obtained from Cell Signaling Technology Inc. (Danvers, MA, USA). Polyclonal rabbit anti-CBP N-terminus and mouse anti-glyceraldehyde 3-phosphate dehydrogenase (GAPDH) were purchased from Millipore (Billerica, MA, USA). Polyclonal rabbit anti-p300 (N-15) came from Santa Cruz Biotechnology Inc. (Santa Cruz, CA, USA). Secondary antibody for western blot detection of GAPDH was obtained from Jackson Immunoresearch Laboratory (West Grove, PA, USA). Alexa Fluor 488 secondary antibody, Alexa Fluor 488 phalloidin and rhodamine phalloidin were purchased from Molecular Probes (Invitrogen, Eugene, OR, USA) and TSA from Calbiochem (EMD Chemicals Inc, Gibbstown, NJ, USA). Texas Red and gentamicin linked to Texas Red (GTTR) were the kind gifts of Dr. Peter Steyger (Oregon Health & Science University, Portland, OR, USA). Type I rat tail collagen was obtained from BD biosciences (San Jose, CA, USA). ECL Plus Western Blotting Detection Reagents were purchased from GE Healthcare UK Limited (Little Chalfont, Buckinghamshire, UK). All other reagents were purchased from Sigma-Aldrich, Inc. (St. Louis, MO, USA).

Animals

Sexually mature male (6 weeks) and female (8 weeks) CBA/J mice were purchased from Harlan Sprague–Dawley Co. (Indianapolis, IN, USA). The animals were maintained on a 12-h light/12-h dark schedule and had free access to water and a regular mouse diet (Purina 5001; Purina, St Louis, MO, USA). For breeding, one male and two female mice were placed in one cage after 1 week of acclimation to their habitat. Experimental protocols were approved by the University of Michigan Committee on the Use and Care of Animals (UCUCA) and animal care was under the supervision of the University of Michigan's Unit for Laboratory Animal Medicine (ULAM).

Organotypic cultures of post-natal organ of Corti

The culture procedures were modified from published reports (Zheng and Gao 1996; Ding *et al.* 2002). In brief, mice of post-natal day 3 (p3) were euthanized after antisepsis with 70% ethanol, and the inner ears were removed. The cochleae were immersed in cold Hank's Balanced Salt Solution and the lateral wall tissues (stria vascularis and spiral ligament) and the auditory nerve bundle were dissected away leaving the organ of Corti and spiral ganglion neurons. The explants were placed onto a previously prepared culture dish (a 15-μL drop of rat tail collagen solution was allowed to polymerize for approximately 15 min on a 35-mm dish) in 1 mL

of culture medium consisting of Basal Medium Eagle, 1% serum-free supplement (Gibco catalogue number 51500-056; Invitrogen, Carlsbad, CA, USA), 1% bovine serum albumin, 5 mg/mL glucose and 10 U/mL penicillin G. The cochlear explants were incubated (37°C, 5% CO_2) for 4 h, and an additional 1 mL of culture medium was added to submerse the explants.

Treatment of organ culture explants

Explants were incubated for two days to allow for recovery from dissection stress before any experiments were begun. The explants were then divided into experimental groups, and the medium was exchanged for new media containing drugs under study and incubated for the desired time points. For the studies of protection, explants were matched: the explant from one ear of an animal received gentamicin only and the explant from the other ear was treated with gentamicin combined with a potential protective agent. Unless otherwise noted, working concentrations were 0.2 mM gentamicin or 6 mM sodium butyrate dissolved in the culture medium. TSA was dissolved in 100% dimethyl sulfoxide (DMSO) and stored at −20°C if necessary. Four μL of a 0.1 mM TSA solution were added to 2 mL of culture medium for final concentrations of 200 nM TSA and 0.2% DMSO. Vehicle control incubations were carried out in the presence of 0.2% DMSO.

Hair cell counts

Explants were fixed with 4% paraformaldehyde overnight at 4°C and permeabilized for 30 min with 3% Triton X-100 in phosphate-buffered saline (PBS) at room temperature (22–24°C). The specimens were then washed three times with PBS and incubated with Alexa 488 phalloidin (1 : 200) or rhodamine-phalloidin (1 : 100) at room temperature (22–24°C) for 30 min. After several rinses in PBS, the specimens were mounted on a slide with GEL/MOUNT™ (Biomeda Corp., Foster City, CA, USA). The phalloidin-stained stereociliary bundles and circumferential F-actin rings on the cuticular plate of outer and inner hair cells allowed the determination of cells that were present or missing. Cell populations were assessed on a Leitz Orthoplan upright microscope equipped for epifluorescence, using a 50× oil immersion objective. The right objective had a 0.17-mm calibrated scale imposed on the field for reference and the single row of inner hair cells and all three rows of outer hair cells were oriented longitudinally within each 0.17-mm frame. Each successive 0.17-mm field was evaluated for the absence of inner and outer hair cells beginning at the apex and moving down the organ of Corti to the base. Cell counts were entered into a computer program (KHRI Cytocochleogram, version 3.0.6, Kresge Hearing Research Institute, University of Michigan, Ann Arbor, MI, USA) for comparison with a normative data base established from control specimens. The percentage of missing hair cells was calculated and plotted as a function of distance from the apical turn to the basal turn of the explant.

Immunofluorescent assessment of organ of Corti explants

Explants were fixed with 4% paraformaldehyde overnight at 4°C and permeabilized for 30 min with 3% Triton X-100 in PBS at room temperature (22–24°C). The specimens were washed three times with PBS and blocked with 10% normal goat serum for 30 min at room temperature (22–24°C), followed by incubation at 4°C for 72 h with the primary antibodies against acetyl-histone H2A (Lys5), acetyl-histone H2B (Lys12), acetyl-histone H3 (Lys 9), acetyl-histone H4 (Lys 8), or polyclonal rabbit anti-HDAC1, diluted 1 : 50 in PBS. After three washes with PBS, a secondary Alexa 488-conjugated goat anti-rabbit antibody was applied at a concentration of 1 : 200 in PBS at 4°C overnight in darkness. For fluorescent visualization of hair cells, the specimens were incubated with rhodamine phalloidin (1 : 100) at room temperature (22–24°C) for 1 h; for visualization of nuclei, the specimens were incubated with Hoechst 33342 (2 μg/mL in PBS) at room temperature (22–24°C) for 30 min. After several rinses in PBS, the specimens were mounted on a slide with GEL/MOUNT™ (Biomeda Corp.). Preparations were observed with a Leica DMIL microscope (Leica Microsystems Inc. Bannockburn, IL, USA) and imaged with an Olympus Fluoview Confocal Laser Scanning Microscope-FV500 (Olympus American, Melville, NY, USA).

Immunostaining of histones was quantified from confocal images taken under identical conditions and equal setting parameters using ImageJ software (National Institute of Health, Bethesda, MD, USA). The fluorescence intensity of nuclei was measured in 0.212-mm segments of the basal portion of the explant, containing about 70 outer and 20 inner hair cells in control preparations. Individual nuclei were localized and counted by outlining the nuclear membrane in the blue Hoechst 33342-stained images, and the fluorescence of anti-acetyl histone staining was analyzed in the corresponding green images. The average fluorescence intensity per nucleus was then calculated, and the relative fluorescence intensity was quantified by normalizing the ratio of average fluorescence intensity of nuclei in treated cells to the average fluorescence of nuclei in control cells. Individual preparations from three animals per condition were examined and data subjected to statistical analysis.

Extraction of total proteins and western blotting

After incubation, explants were washed with PBS and eight explants were pooled and homogenized in ice cold ristocetin-induced platelet agglutination lysis buffer by using a glass/glass micro tissue grinder for 30 s. Subsequently, tubes were sonicated in an ultrasonic water bath for 15 s. After 30 min on ice, insoluble material was removed at 12 000 *g* at 4°C for 10 min and the supernatants were stored at −80°C until analysis.

Protein concentrations were determined using the Bio-Rad Protein Assay dye reagent (Bio-Rad, Hercules, CA, USA) with bovine serum albumin as a standard, and samples of 40 μg each were separated by sodium dodecyl sulfate–polyacrylamide gel electrophoresis. After electrophoresis, the proteins were transferred onto nitrocellulose membrane (Pierce, Rockford, IL, USA) and blocked with 5% non-fat dry milk in PBS with 0.1% Tween 20 (PBS-T). The membranes were incubated with primary antibodies rabbit anti-HDAC1 (1 : 1000), anti-HDAC3 (1 : 1000), anti-HDAC4 (1 : 1000), anti-HDAC6 (1 : 1000), anti-Histone H2A (1 : 1000) and anti-Histone H3 (1 : 1000), anti-CBP NT (1 : 3000), and anti-p300 (1 : 300) or mouse anti-GAPDH (1 : 10 000) in 5% skim milk in PBS-T overnight at 4°C, and then washed three times (10 min each) with PBS-T. Membranes were incubated with an appropriate secondary antibody at a concentration of 1 : 1000 (Cell Signaling Technology Inc.), or 1 : 10 000 (Jackson Immunoresearch Laboratory) for 1 h at room temperature (22–24°C). Following extensive washing of the

membrane, the immunoreactive bands were visualized by enhanced chemiluminescence.

Scans of western blots were analyzed using AlphaEase software SpotDenso tool (Alpha Innotech, San Leandro, CA, USA). The band densities were first normalized to background, then the ratio of the selected proteins to GAPDH (run on the same gel) was calculated. Finally, the difference in relative densities of the control and experimental bands was tested for statistical significance using Primer of Biostatistics software (McGraw-Hill Software, New York, NY, USA).

Gentamicin uptake

Explants were incubated with serum-free medium containing 1.56 μg/mL Texas Red dye, 1.56 μg/mL GTTR (Myrdal *et al.* 2005), or 1.56 μg/mL GTTR plus 200 nM TSA for 8 h. After fixation and permeabilization as described for immunofluorescence of explants, the specimens were incubated with Alexa Fluor 488 phalloidin (1 : 100) for 1 h and Hoechst 33342 (2 μg/mL in PBS) for 30 min for fluorescent visualization of hair cell F-actin and nuclei, respectively, and the assessment of gentamicin fluorescence.

Statistical analysis

Data were statistically evaluated by Student's *t*-test and by analyses of variance with Student–Newman–Keuls test for significance ($p < 0.05$) using Primer of Biostatistics software (McGraw-Hill Software). For the relative fluorescence intensity, a two tailed one-sample *t*-test using GraphPad Software (GraphPad Software Inc., San Diego, CA, USA) was applied.

Results

Gentamicin-induced hair cell loss in mouse organ of Corti organotypic cultures

Explants of the organ of Corti of the post-natal day 3 mouse, cultured for an additional 3 days (Fig. 1a), were approxi-

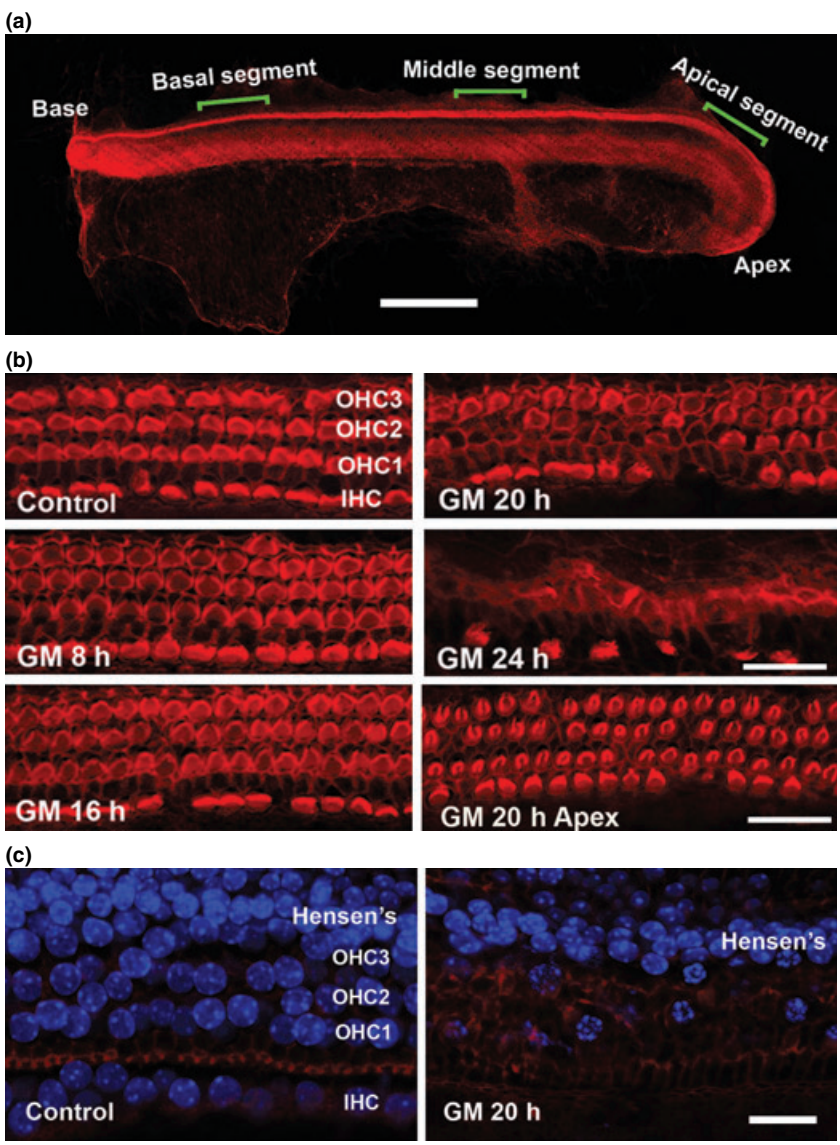

Fig. 1 Gentamicin-induced hair cell loss in mouse organotypic cultures of the organ of Corti. (a) A whole mount of the organ of Corti explanted at post-natal day 3 and maintained in culture for 2 days was stained for F-actin with rhodamine phalloidin (red fluorescence). The outer stained perimeter contains the hair cell layer. Basal, middle and apical segments indicate the approximate areas analyzed in this study. Scale bar = 500 μm. (b) Base-to-apex gradient of hair cell loss. Surface preparations of the basal segment show the outlines of inner and outer hair cells stained for F-actin with rhodamine phalloidin. Control incubations in the absence of gentamicin maintained a normal appearance at 24 h. In the basal segment of the organ of Corti, outer hair cell loss began after 16 h of incubation with gentamicin and progressed with increasing time while outer hair cells at the apex (GM 20 h Apex) remained intact. The images are representative of eight individual preparations at each time point. Scale bar = 20 μm. (c) Hensen's cells remained intact after treatment with 0.2 mM gentamicin for 20 h. Nuclei are stained blue with Hoechst 33342 and Hensen's cells are identified by their position on the surface preparation and in comparison with remaining hair cells stained for F-actin. GM, gentamicin; IHC, inner hair cells; OHC1, OHC2, OHC3, outer hair cells of the first, second and third row, respectively. Scale bar = 20 μm.

mately 4.25 mm long and contained a total of about 2100 outer hair cells in three rows and 700 inner hair cells. Actions of gentamicin were mostly analyzed in basal segments, the primary location of its ototoxic action while middle and apical segments of the preparation were additionally evaluated for gentamicin uptake.

In control preparations, incubated for 24 h in culture medium, hair cells were well preserved (Fig. 1b). With 0.2 mM gentamicin, the explants showed loss of neither inner nor outer hair cells after 8 h (and 12 h, not shown) and only minimal loss in the basal segment at 16 h. Hair cell death became evident by 20 and 24 h but cells in the most apical area were spared. In contrast to its toxicity towards hair cells, gentamicin did not destroy non-sensory cells (Hensen's cells; Fig. 1c).

Quantitative evaluation of surface preparations of the entire length of the organ of Corti confirmed that hair cell loss increased with increasing concentrations of gentamicin (Fig. 2). A loss of 50% of hair cells was reached at a concentration of about 150 μM gentamicin.

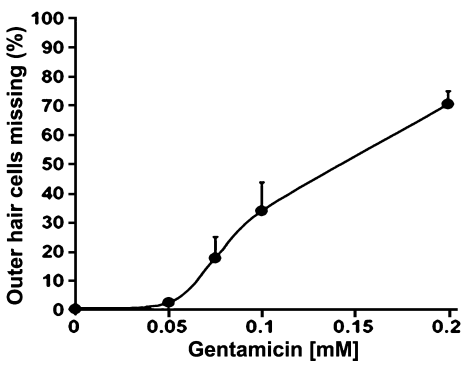

Fig. 2 Dose-dependence of outer hair cell loss. Surface preparations of the entire length of the explant were evaluated quantitatively for hair cell loss as described in 'Methods'. After 24 h of incubation the percentage of missing outer hair cells increases with increasing doses of gentamicin. Data are presented as means ± SD. Percent of hair cells missing at gentamicin concentrations > 0.05 mM is significantly different ($p < 0.05$) from controls. Controls, $n = 7$; 0.05 mM, $n = 3$; 0.075 mM, $n = 5$; 0.1 mM, $n = 15$; 0.2 mM, $n = 9$.

Gentamicin reduces histone acetylation in outer hair cells and the histone deacetylase inhibitor trichostatin A blocks this action

Acetylation of the histone core proteins H2A, H2B, H3, and H4 decreased significantly in both outer and inner hair cells after incubation with 0.2 mM gentamicin for 8 h and stayed at reduced levels by 16 and 20 h (Fig. 3). The amount of total (acetylated plus non-acetylated) histone protein, measured by western blotting for H2A and H3, remained unchanged by gentamicin treatment (data not shown). TSA alone initially increased acetylation of all core histones in inner and outer hair cells with H2B and H4 showing a considerably larger response than H3 and H2A. Except for H2A, the single dose of TSA maintained higher than normal acetylation levels through 20 h. When combined with gentamicin, TSA initially maintained acetylation of all core histones at near control levels, but its effect was diminished by 20 h in most cases. In contrast to hair cells, the acetylation of histones in Hensen's cells did not change with gentamicin treatment. This was most evident in the 20 h-incubations where the staining for acetyl histones in Hensen's cell nuclei is seen above the rows of largely missing outer hair cells.

Gentamicin transiently increases histone deacetylases in outer hair cells

In order to probe into the reasons for the decreased histone acetylation, we determined protein levels of representative deacetylases HDAC1 and HDAC3 (class I HDAC), HDAC4, and HDAC6 (class II HDAC), and representative acetyltransferases CBP and p300 by western blot (Fig. 4a and c). Treatment of explants with 0.2 mM gentamicin for 8 h resulted in significant elevations of HDAC1, HDAC3, and HDAC4, while HDAC6 remained stable. In contrast to

Fig. 3 (a–d) Acetylation of histone core proteins in both outer and inner hair cells is decreased by gentamicin and restored by trichostatin A. Explants received the treatments as stated below and were stained (green) by immunocytochemistry for histone H2A Ack5 (a); histone H2B Ack12 (b); histone H3 Ack9 (c); or histone H4 Ack8 (d). Red stain is rhodamine phalloidin for F-actin in hair cells; blue is Hoechst 33342 staining of nuclei. The figures are representative images of three individual preparations of the basal segment of the organ of Corti for each condition. Vehicle, 0.2% DMSO; TSA, 200 nM TSA with 0.2% DMSO. GM, gentamicin; IHC, inner hair cells; OHC1, outer hair cell first row; OHC2, outer hair cell second row; OHC3, outer hair cell third row. Scale bars = 20 μm. Left panels (a–d): Explants were treated with 200 nM TSA for the times indicated on the images. 'Vehicle' denotes control incubation with 0.2% DMSO for 8 h. Acetylation of histone is increased in the presence of TSA compared to the vehicle only. Middle panels (a–d): Explants were treated with 0.2 mM gentamicin for the times indicated on the images. Acetylation of all histones in both outer and inner hair cells decreased in a time-dependent manner as compared to an 8-h incubation in control medium. Right panels (a–d): Explants received both 0.2 mM gentamicin and 200 nM TSA for the times indicated on the images. Histone acetylation in both outer and inner hair cells is maintained near control levels for the first 8 h (16 h in the case of H3) of incubation but decreases at later times. Graphs of relative fluorescence intensity in both outer and inner hair cells obtained from the immunocytochemical images as described in Methods section are placed next to the corresponding fluorescence panel. Histone acetylation shows similar patterns but quantitative differences in response to gentamicin and TSA. Data are means ± SD. Significance of differences: $^{*}p < 0.05$ vs. control; $^{**}p < 0.01$ vs. control.

HDACs, levels of the acetyltransferases CBP and p300 remained unaffected by gentamicin treatment (Fig. 4c).

Since the extracts from whole explants contain protein from sensory (hair) cells, supporting cells and nerve endings, immunocytochemistry was used to ascertain the cellular localization of the changes in HDAC levels. Employing HDAC1 as a marker (Fig. 4b), transiently increased fluorescence intensity was found in the nuclei of inner and outer hair cells.

Histone deacetylase inhibitors protect against gentamicin-induced hair cell loss

A single application of 200 nM TSA protected against gentamicin-induced loss of inner and outer hair cells (Fig. 5).

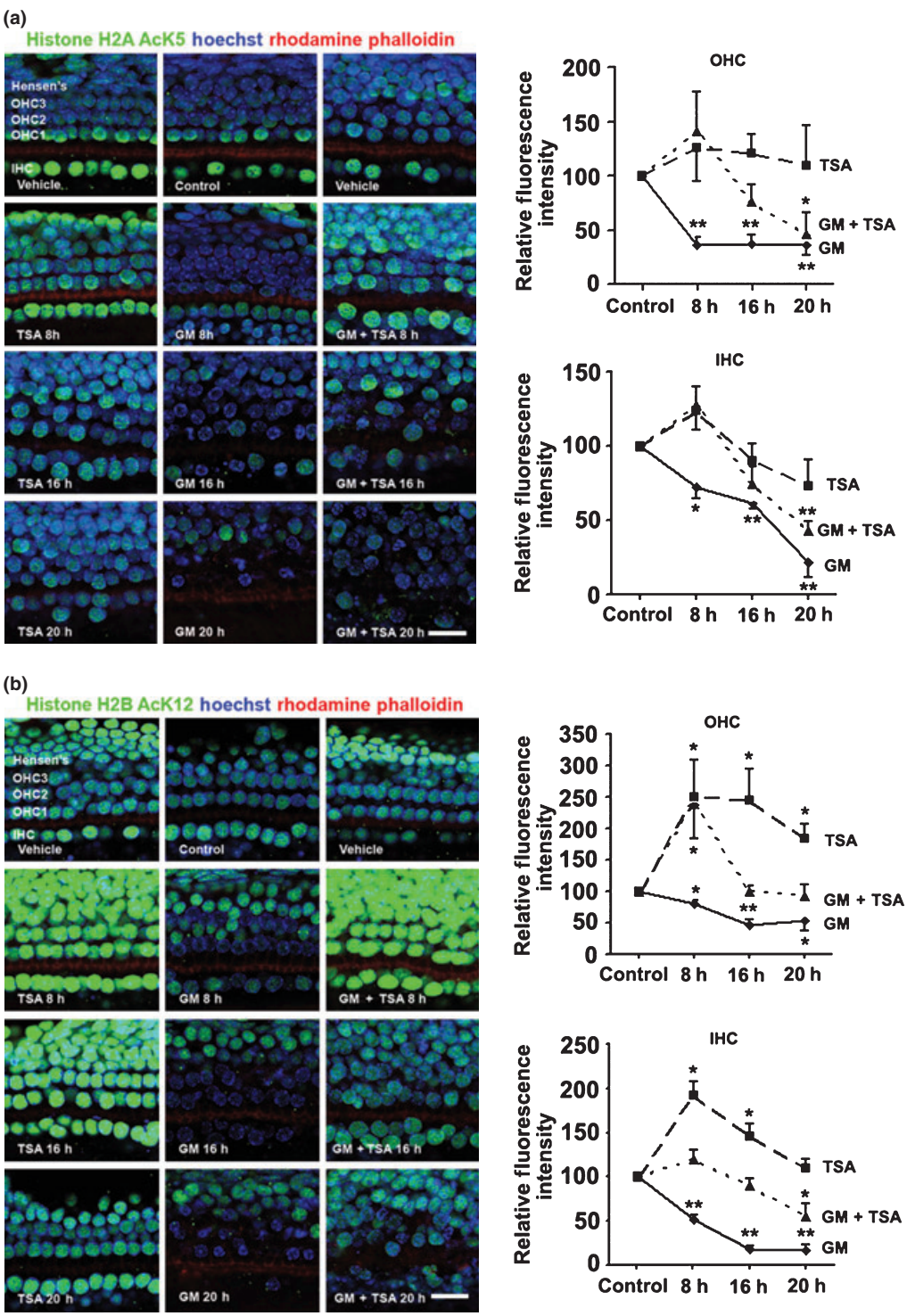

In the basal segment of the explant (Fig. 5a), 0.2 mM gentamicin eliminated most outer hair cells within 20 h while the additional presence of TSA largely preserved their normal appearance. TSA by itself exhibited no toxicity. Since TSA was dissolved in 0.2% DMSO, controls and gentamicin incubations also contained this vehicle.

Assessment of hair cell morphology along the entire explant confirmed the base-to-apex gradient of gentamicin

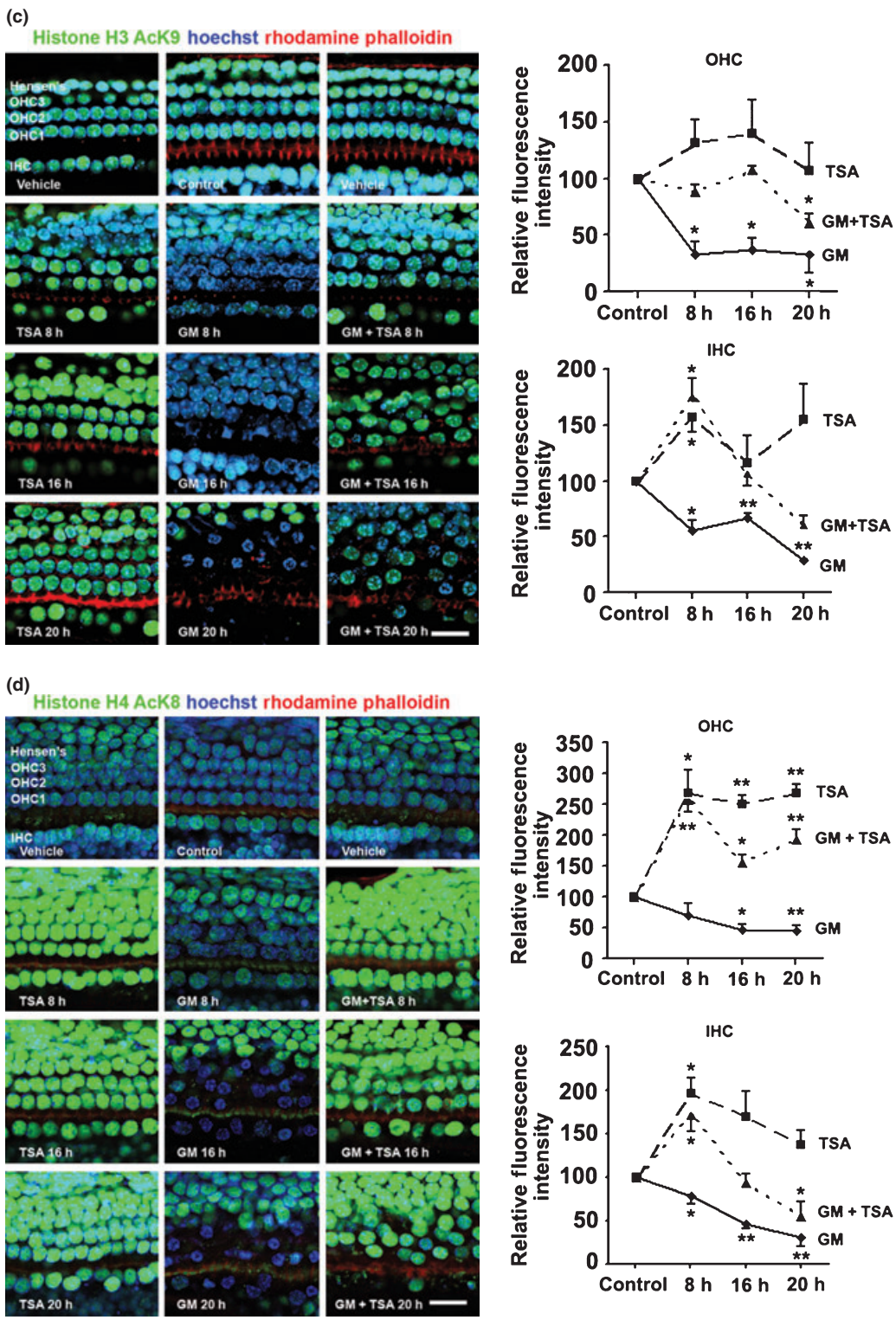

Fig. 3 (Continued)

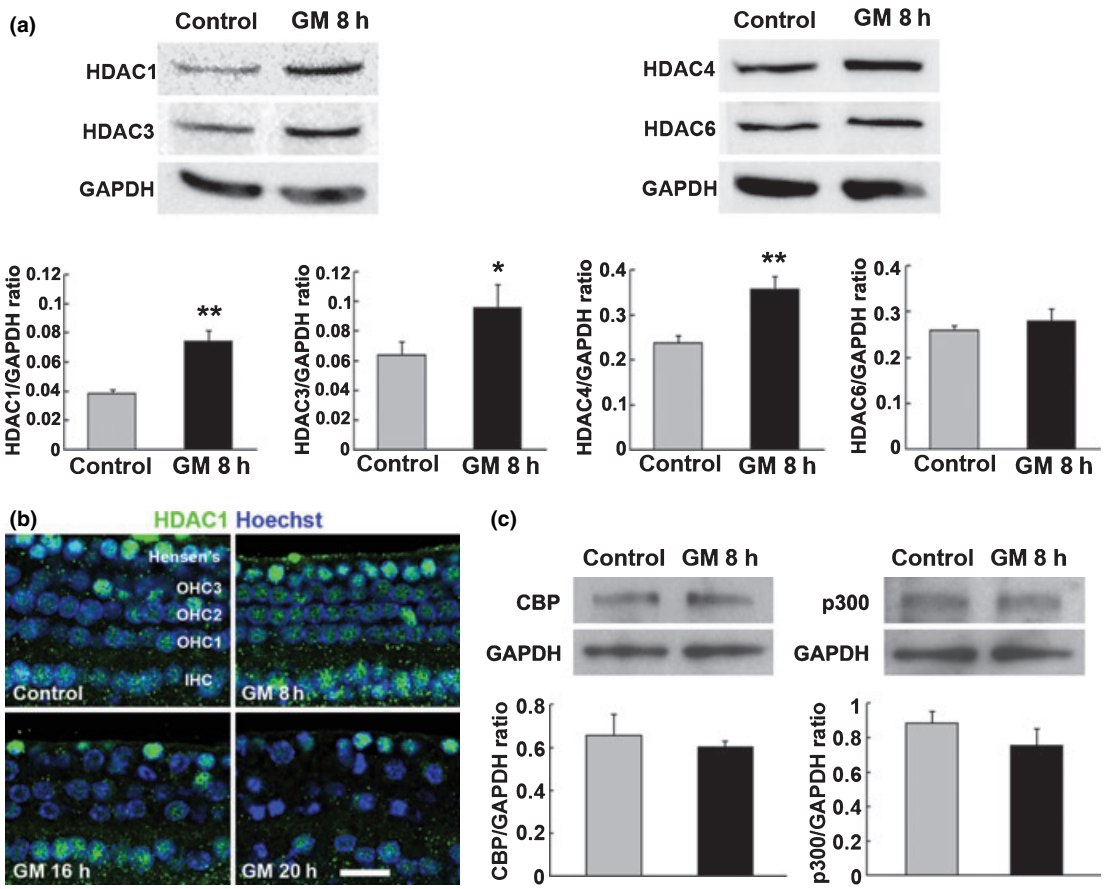

Fig. 4 Histone deacetylases are transiently up-regulated by gentamicin. (a) Western blots detected histone deacetylases-1, -3, -4 and -6 in homogenates of organ of Corti explants. Membranes were sequentially stained for HDAC1 and HDAC3 and for HDAC4 and HDAC6. Significance of differences: $^{*}p < 0.05$, $^{**}p < 0.01$ compared to the corresponding control groups ($n = 3$, means ± SD). (b) Immunocytochemistry of organ of Corti explants for HDAC 1 (green) indicated a transient increase in outer hair cells at 8 h of gentamicin treatment. Blue is Hoechst 33342 staining for nuclei. The figure shows representative images from the basal turn of the organ of Corti ($n = 3$ at each time point). Scale bar = 20 μm. (c) Western blots detected histone acetylases CBP and p300 in homogenates of organ of Corti explants. There was no difference between controls and gentamicin-treated explants ($n = 3$, means ± SD). GM, gentamicin; IHC, inner hair cell; OHC, outer hair cells; OHC1, outer hair cell first row; OHC2, outer hair cell second row; OHC3, outer hair cell third row.

toxicity. Loss of both outer and inner hair cells was almost complete at the base while the apex was spared. In the protection experiments, the contributions of DMSO and TSA had to be differentiated. The solvent DMSO is a radical scavenger and attenuated outer hair cell loss in the middle sections and inner hair cells at the very base (Fig. 5b), an observation in agreement with previous reports of DMSO protection *in vivo* (Sha and Schacht 1998). The additional presence of TSA significantly reduced the loss of both inner and outer hair cells beyond the attenuation by DMSO. No loss of outer hair cells was apparent from the apex to the middle of the organ of Corti and a maximal 50% loss was seen in the base. Inner hair cell loss was attenuated uniformly from base to apex by TSA when compared to incubations with DMSO.

Sodium butyrate (6 mM), a water-soluble histone deacetylase inhibitor had a similar, albeit weaker, protective effect on gentamicin-induced hair cell loss (Fig. 5c). Protection of outer hair cells was best in the apical and middle region and absent from the very base, the most severely damaged region. Inner hair cell survival was less attenuated. Sodium butyrate alone did not cause any hair cell loss.

Quantitative evaluation of hair cell loss for the entire length of the explant confirmed significant protection of both inner and outer hair cells (Fig. 5d). The presence of TSA, in comparison to incubations of gentamicin with its vehicle DMSO alone, essentially doubled the number of surviving inner hair cells and increased survival of outer hair cells to over 90%. Sodium butyrate increased survival of both cell types by 60–70%.

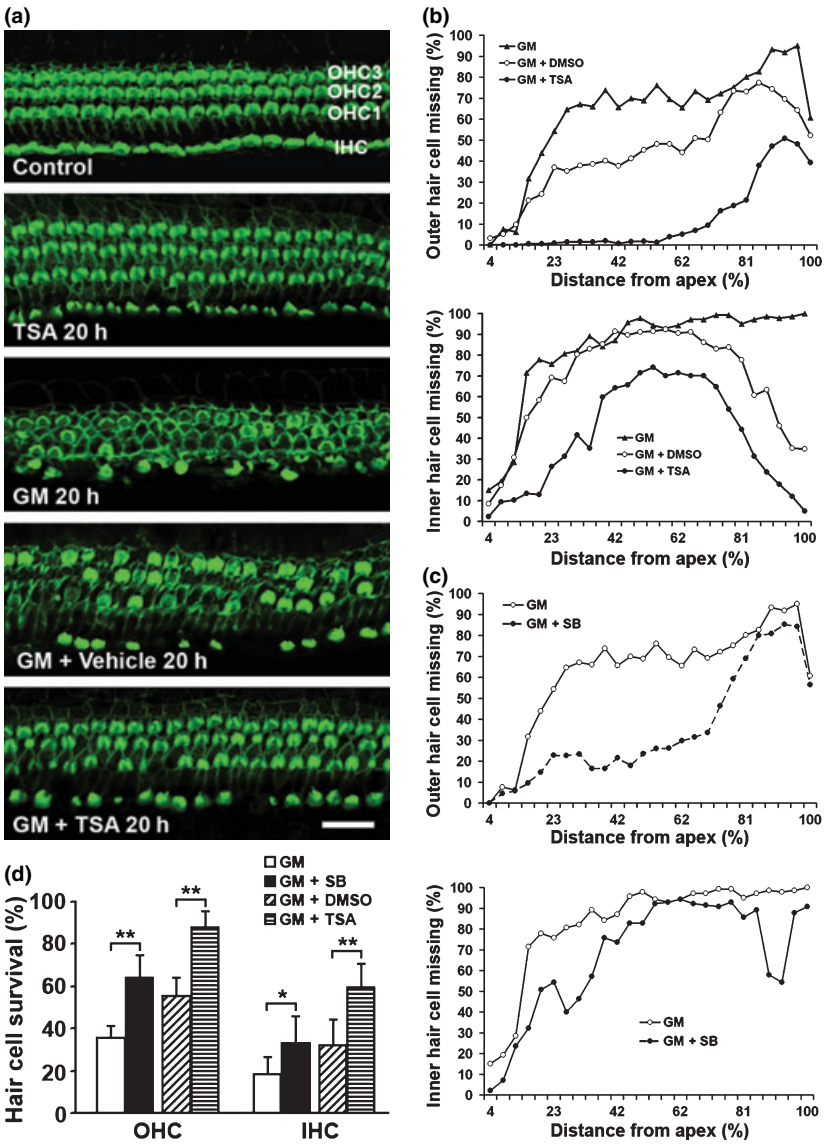

Fig. 5 Histone deacetylase inhibitors protect against gentamicin-induced hair cell loss. (a) Representative images from the basal segment of the organ of Corti after 20 h of incubation, showing the outline of hair cells stained with Alexa 488 phalloidin. Control: incubation with 0.2% DMSO; TSA: 200 nM TSA dissolved in 0.2% DMSO; GM 20 h: explant treated with 0.2 mM gentamicin for 20 h; GM + vehicle: 0.2 mM gentamicin plus 0.2% DMSO; GM + TSA: 0.2 mM gentamicin plus 200 nM TSA dissolved in 0.2% DMSO. $n = 8$ for each condition. Scale bar = 20 μm. (b) Quantitative evaluation of loss of outer and inner hair cells along the entire length of the organ of Corti explant after 20 h of incubation with gentamicin in the absence or presence of 200 nM TSA. There is no loss of inner or outer hair cells in control incubations with sodium sulfate (0.5 mM) substituting for gentamicin sulfate or with DMSO alone. $n = 8$ for each condition. (c) Quantitative evaluation of loss of outer and inner hair cells along the entire length of the organ of Corti explant after 20 h of incubation with gentamicin in the absence or presence of 6 mM sodium butyrate. $n = 8$ for each condition. (d) Average hair cell survival under treatment with gentamicin and co-treatment with inhibitors or vehicle ($n = 8$, means ± SD. $^*p < 0.05$, $^{**}p < 0.01$). GM, gentamicin; IHC, inner hair cells; OHC, outer hair cells; SB, sodium butyrate; TSA, trichostatin A.

Trichostatin A does not interfere with gentamicin uptake into hair cells

Uptake of gentamicin into organ cultures was monitored with the drug tagged to fluorescent Texas Red (GTTR). GTTR efficiently entered cochlear cells and was evident after 8 h of incubation in inner and outer hair cells as well as in Hensen's cells from base to apex (Fig. 6a). TSA did not influence this uptake (Fig. 6b), as confirmed by quantitative evaluation of immunofluorescence (not shown). Free Texas Red at comparable concentrations served as a control and did not enter the tissue.

Discussion

Epigenetic changes, aberrant covalent modifications of DNA or histone core proteins, have increasingly become recognized as causes of or contributions to disease pathogenesis (Lu *et al.* 2006; Bhaumik *et al.* 2007). Histone acetylation imbalance is linked to transcriptional dysfunction, gene silencing and the development of neurodegenerative disorders. We propose here that it is involved in the death of inner ear sensory cells by aminoglycoside antibiotics.

The explant of the organ of Corti shows the preferential loss of outer hair cells in response to as little as 75 μM gentamicin and a base-to-apex progression of damage that is characteristic of aminoglycoside actions on the cochlea in both human and experimental animals including the mouse (Forge and Schacht 2000; Wu *et al.* 2001). The fact that supporting cells such as Hensen's cells are spared also agrees with *in-vivo* observations and is best explained by the intrinsic susceptibility of hair cells to conditions that generate oxidative stress (Sha *et al.* 2001). Compared to the *in-vivo*

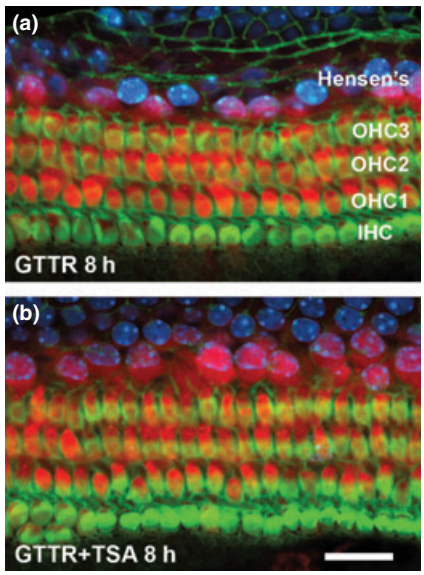

Fig. 6 Trichostatin A does not affect gentamicin uptake into outer hair cells. Explants were incubated for 8 h with 1.56 μg/mL gentamicin tagged with Texas Red (GTTR) in the absence (a) or presence (b) of 200 nM TSA. Red fluorescence is GTTR, green fluorescence is staining for F-actin in stereocilia of hair cells with Alexa 488-phalloidin, blue is Hoechst 33342 for nuclei. Images show a basal segment and are representative of three incubations under each condition. Scale bar = 20 μm.

situation, however, the time course of hair cell loss is accelerated, making explants an excellent model to probe mechanisms of drug ototoxicity in which hair cell death can be conveniently observed and manipulated (Zhang *et al.* 2003; Tabuchi *et al.* 2007).

The gentamicin-induced demise of the sensory cells is evident in the explant within 16–24 h after exposure to the drug. Histone acetylation begins to decrease at 8 h in inner and outer hair cells prior to their death but does not decrease at all in Hensen's cells which remain unaffected by gentamicin. This timing and location suggest that the change in histone acetylation may be one of the triggers to cell loss. The decrease encompasses the four histone core proteins suggesting a global action of the drug, which can easily be explained by the up-regulation of HDACs during gentamicin treatment. The differential action of gentamicin on HDACs offers speculation as to the potential downstream consequences of gentamicin-induced histone deacetylation. HDACs target histone protein substrates acting as transcription repressors but they also target non-histone substrates such as hormone receptors, chaperone proteins and cytoskeleton proteins, which regulate cell proliferation and cell death (Xu *et al.* 2007). Of the different types of HDACs tested here, it is HDAC6 that preferentially targets non-histone substrates, including α tubulin and HSP90 (Kawaguchi *et al.* 2003). The fact that gentamicin altered the levels of HDAC1, -3 and -4, but not of HDAC6 suggests an interference with the acetylation of histone proteins that are involved in the regulation of gene expression.

It is interesting to note that the imbalance in histone acetylation appears to be caused by an increase in HDACs without a change in HATs. Most commonly, loss of HAT activity rather than an increase in HDAC activity is observed in disorders associated with a compromised acetylation homeostasis (Saha and Pahan 2006). The action of aminoglycoside antibiotics could thus constitute a novel mechanism towards acetylation imbalance which deserves further detailed investigation.

Compelling evidence for a causal involvement of histone deacetylation in cell death comes from the evidence that the HDAC inhibitor TSA restores the acetylation balance with a consequent preservation of hair cells. This notion is further supported by the facts that TSA does not influence the uptake of gentamicin into cells (which could mimic 'protection') and that another HDAC inhibitor, sodium butyrate, likewise acts in a protective manner. Both inhibitors are more efficient at preserving outer hair cells than inner hair cells but even outer hair cell protection is partial and could indicate a delay rather than an outright blocking of cell death. This latter fact, however, is well correlated with the pattern of histone acetylation which is limited in time presumably because of the diminishing inhibitor effectiveness in the incubation (Siavoshian *et al.* 2000; Elaut *et al.* 2007). Finally, rescue by sodium butyrate from ototoxic damage has also been reported for the anticancer drug cisplatin, whose primary targets include the outer hair cells (Drottar *et al.* 2006), so that the possibility of a common final pathway of ototoxic damage to sensory cells arises.

Invoking histone deacetylation in aminoglycoside-induced sensory cell death has potential translational consequences. Several HDAC inhibitors have already been approved for clinical use and others are in clinical trials (Glaser 2007). Such inhibitors could benefit the large population of patients that receive aminoglycoside antibiotics for emergency treatment, against tuberculosis, or as prophylaxis in cystic fibrosis and all of whom are at risk for irreversible hearing and balance deficits (Forge and Schacht 2000). The observation that even dietary supplements can change HDAC activities (Dashwood and Ho 2007) may make a protective treatment accessible to patients in developing countries where aminoglycoside use is widespread and expensive medications are not affordable.

Acknowledgement

This study was supported by research grant DC-03685 and core grant P30 DC-05188 from the National Institute on Deafness and Other Communication Disorders, NIH.

Disclosure statement

There are no conflicts of interest for any of the authors. The data contained in the manuscript have not been previously published, have not been submitted elsewhere, and will not be submitted elsewhere while under review. All experimental protocols were approved by the University of Michigan Committee on Use and Care of Animals and animal care was supervised by the University of Michigan's Unit for Laboratory Animal Medicine. All authors have reviewed the contents of the manuscript, approve of its contents, and validate the accuracy of the data.

References

Bhaumik S. R., Smith E. and Shilatifard A. (2007) Covalent modifications of histones during development and disease pathogenesis. *Nat. Struct. Mol. Biol.* **14**, 1008–1016.

Dashwood R. H. and Ho E. (2007) Dietary histone deacetylase inhibitors: from cells to mice to man. *Semin. Cancer Biol.* **17**, 363–369.

Ding D., Stracher A. and Salvi R. J. (2002) Leupeptin protects cochlear and vestibular hair cells from gentamicin ototoxicity. *Hear. Res.* **164**, 115–126.

Drottar M., Liberman M. C., Ratan R. R. and Roberson D. W. (2006) The histone deacetylase inhibitor sodium butyrate protects against cisplatin-induced hearing loss in guinea pigs. *Laryngoscope* **116**, 292–296.

Elaut G., Laus G., Alexandre E., Richert L., Bachellier P., Tourwe D., Rogiers V. and Vanhaecke T. (2007) A metabolic screening study of trichostatin A (TSA) and TSA-like histone deacetylase inhibitors in rat and human primary hepatocyte cultures. *J. Pharmacol. Exp. Ther.* **321**, 400–408.

Fischer A., Sananbenesi F., Wang X., Dobbin M. and Tsai L. H. (2007) Recovery of learning and memory is associated with chromatin remodelling. *Nature* **447**, 178–182.

Forge A. and Schacht J. (2000) Aminoglycoside antibiotics. *Audiol. Neurootol.* **5**, 3–22.

Gao L., Cueto M. A., Asselbergs F. and Atadja P. (2002) Cloning and functional characterization of HDAC11, a novel member of the human histone deacetylase family. *J. Biol. Chem.* **277**, 25748–25755.

Glaser K. B. (2007) HDAC inhibitors: clinical update and mechanism-based potential. *Biochem. Pharmacol.* **74**, 659–671.

Hainrichson M., Nudelman I. and Baasvo T. (2008) Designer aminoglycosides: the race to develop improved antibiotics and compounds for the treatment of human genetic diseases. *Org. Biomol. Chem.* **21**, 227–239.

Hermann C. (2007) Review: variability of host-pathogen interaction. *J. Endotoxin Res.* **13**, 199–218.

Jiang H., Sha S.-H. and Schacht J. (2005) The NF-κB pathway protects cochlear hair cells from aminoglycoside-induced ototoxicity. *J. Neurosci. Res.* **79**, 644–651.

Jiang H., Sha S. H. and Schacht J. (2006a) Kanamycin alters cytoplasmic and nuclear phosphoinositide signaling in the organ of Corti *in vivo*. *J. Neurochem.* **99**, 269–276.

Jiang H., Sha S. H., Forge A. and Schacht J. (2006b) Caspase-independent pathways of hair cell death induced by kanamycin *in vivo*. *Cell Death Differ.* **13**, 20–30.

Kawaguchi Y., Kovacs J. J., McLaurin A., Vance J. M., Ito A. and Yao T. P. (2003) The deacetylase HDAC6 regulates aggresome formation and cell viability in response to misfolded protein stress. *Cell* **115**, 727–738.

Kim H. J., Rowe M., Ren M., Hong J. S., Chen P. S. and Chuang D. M. (2007) Histone deacetylase inhibitors exhibit anti-inflammatory and neuroprotective effects in a rat permanent ischemic model of stroke: multiple mechanisms of action. *J. Pharmacol. Exp. Ther.* **321**, 892–901.

Lu Q., Qiu X., Hu N., Wen H., Su Y. and Richardson B. C. (2006) Epigenetics, disease, and therapeutic interventions. *Ageing Res. Rev.* **5**, 449–467.

Marks P. A., Richon V. M., Breslow R. and Rifkind R. A. (2001) Histone deacetylase inhibitors as new cancer drugs. *Curr. Opin. Oncol.* **13**, 477–483.

Marks P. A., Richon V. M., Miller T. and Kelly W. K. (2004) Histone deacetylase inhibitors. *Adv. Cancer Res.* **91**, 137–168.

Morrison B. E., Majdzadeh N., Zhang X., Lyles A., Bassel-Duby R., Olson E. N. and D'Mello S. R. (2006) Neuroprotection by histone deacetylase-related protein. *Mol. Cell. Biol.* **26**, 3550–3564.

Myrdal S. E., Johnson K. C. and Steyger P. S. (2005) Cytoplasmic and intra-nuclear binding of gentamicin does not require endocytosis. *Hear. Res.* **204**, 156–169.

de Ruijter A. J., van Gennip A. H., Caron H. N., Kemp S. and van Kuilenburg A. B. (2003) Histone deacetylases (HDACs): characterization of the classical HDAC family. *Biochem. J.* **370**, 737–749.

Sadri-Vakili G. and Cha J. H. (2006) Mechanisms of disease: histone modifications in Huntington's disease. *Nat. Clin. Pract. Neurol.* **2**, 330–338.

Saha R. N. and Pahan K. (2006) HATs and HDACs in neurodegeneration: a tale of disconcerted acetylation homeostasis. *Cell Death Differ.* **13**, 539–550.

Sha S.-H. and Schacht J. (1998) Are aminoglycoside antibiotics excitotoxic? *Neuroreport* **9**, 3893–3895.

Sha S.-H., Taylor R., Forge A. and Schacht J. (2001) Differential vulnerability of basal and apical hair cells is based on intrinsic susceptibility to free radicals. *Hear. Res.* **155**, 1–8.

Siavoshian S., Segain J. P., Kornprobst M., Bonnet C., Cherbut C., Galmiche J. P. and Blottiere H. M. (2000) Butyrate and trichostatin A effects on the proliferation/differentiation of human intestinal epithelial cells: induction of cyclin D3 and p21 expression. *Gut* **46**, 507–514.

Tabuchi K., Pak K., Chavez E. and Ryan A. F. (2007) Role of inhibitor of apoptosis protein in gentamicin-induced cochlear hair cell damage. *Neuroscience* **149**, 213–222.

Taylor J. P. and Fischbeck K. H. (2002) Altered acetylation in polyglutamine disease: an opportunity for therapeutic intervention? *Trends Mol. Med.* **8**, 195–197.

Wu W. J., Sha S. H., McLaren J. D., Kawamoto K., Raphael Y. and Schacht J. (2001) Aminoglycoside ototoxicity in adult CBA, C57BL and BALB mice and the Sprague-Dawley rat. *Hear. Res.* **158**, 165–178.

Xu W. S., Parmigiani R. B. and Marks P. A. (2007) Histone deacetylase inhibitors: molecular mechanisms of action. *Oncogene* **26**, 5541–5552.

Zhang M., Liu W., Ding D. and Salvi R. (2003) Pifithrin-alpha suppresses p53 and protects cochlear and vestibular hair cells from cisplatin-induced apoptosis. *Neuroscience* **120**, 191–205.

Zheng J. L. and Gao L. (1996) Differential damage to auditory neurons and hair cells by ototoxins and neuroprotection by specific neurotrophins in rat cochlear organotypic cultures. *Eur. J. Neurosci.* **8**, 1897–1905.

